The Impact of Random Dopant Aggregation in Source and Drain on the Performance of Ballistic DG Nano-MOSFETs: A NEGF Study

Antonio Martinez, John R. Barker, Alexei Svizhenko, M. P. Anantram, and Asen Asenov, *Member, IEEE*

***Abstract*—We have studied the effect of deviations from doping uniformity in source and drain on the performance of sub-20 nm silicon double-gate MOSFET devices. The study is motivated by recent direct observation of such inhomogeneities in small MOSFET devices. The model assumes a continuous charge distribution with randomly located regions of high doping. Individual dopants are not resolved. Impurity scattering in the source and drain regions is neglected. The current–voltage characteristics $I_D - V_G$ are computed for devices that differ only in the microscopic arrangement of the randomly distributed high doping regions. We have also studied devices that differ in the number of these clusters. An ensemble of devices with fluctuating numbers of clusters has been constructed based on a Gaussian distribution centered on the mean cluster number derived from the average doping concentration in the source/drain. The impact of high doping clusters, particularly on charge injection, has been studied in detail for the first time using full quantum simulation based on the 2-D nonequilibrium Green function approach coupled self-consistently to Poisson's equation. We have assumed an average lateral symmetry for the double-gate MOSFET. Therefore, we only consider inhomogeneities in doping in the plane of the simulation. The devices studied have 12 nm channel lengths which allows the approximation of ballistic quantum transport through the self-consistent electrostatic potential landscape of the device. The computed current–voltage characteristics are monotonic and they are most strongly affected by the fluctuations in the total number of high doping regions. Fluctuations in the spatial configuration of clusters have a lesser effect. Threshold voltages shifts around 100 mV and on-current fluctuations around 50% are obtained from the simulations. However, the subthreshold slope remains almost independent of the microscopic cluster distribution. The on-current variations are considerably larger than those predicted from classical modeling.**

***Index Terms*—Clustering of dopants, DG-MOSFET, nonequilibrium Green functions.**

I. Introduction

As THE International Technology Roadmap for Semiconductors (ITRS) [1] unfolds, the standard bulk MOSFET architecture will inevitably be replaced by alternative architectures such as double-gate (DG) or silicon-on-insulator (SOI) MOSFETs in order to suppress short channel. However, fluctuations in the discreteness of the dopants in the source/drain, stray dopants in the channel [2], and imperfections in the Si/SiO_2 interface [3] became very important in nanometer-scale devices. The effects of random dopants, doping inhomogeneities, and surface roughness do not average on such small scales [2], [4], [5]. Therefore, the particular configuration of inhomogeneity from device to device produces fluctuations in the current and threshold voltage in an ensemble of technologically similar devices. One critical feature of nanoscaled devices is thus the occurrence of strong performance variations between devices that have macroscopically identically doping. The problem arises because doping is only controllable macroscopically, whereas the discrete microscopic dopant distributions are uncontrolled. Previous studies have drawn attention to problems arising from the presence of small numbers of discretely resolved dopants in the channel of a device: the atomistic doping problem. In the present paper we distinguish doping distributions in source and drain that may be treated as essentially continuous but inhomogeneous in space. The characteristics of such inhomogeneities are modeled by reference to recent direct experimental data [19] on small MOSFETs which has revealed that the source and drain regions show random extensions in the vicinity of the channel in which random dopant aggregations, or clusterings, occur (see Fig. 1). Although these clusters are countable, they do not correspond to spatially resolved individual dopant atoms. Their effect is to modify the self-consistent electrostatic potential within the device on a mesoscopic rather than microscopic scale. We are therefore not concerned with the contribution of the microscopic atomic distribution of dopant atoms on scattering in the channel (in classical terms we neglect mobility variations in source and drain). From this point of view it is the influence of clustering on charge injection into the nominally undoped channel that is of interest.

The significance of random dopants for device variability and design was first emphasized in a seminal classical study by Keyes [6]. The first detailed classical and quantum transport studies of the impact of discretely distributed ionized donors on electron transport were reported for electron waveguides and quantum point contacts in semiconductor heterostructure devices [7]–[9] using 2-D models. The influence of the random potential landscape was shown to imply considerable fluctuations in device parameters between devices and strong mobility degradation. The same considerations carry over to MOSFETs in the near ballistic regime [2]–[5]. However, until recently,

Manuscript received June 10, 2006; revised December 20, 2006. This work was supported in part by the EPRSC through grant awards and a Platform grant.

A. Martinez, J. R. Barker, and A. Asenov are with the Electrical Engineering Department, University of Glasgow, Glasgow G12 8LT, U.K. (e-mail: jbarker@elec.gla.ac.uk).

A. Svizhenko was with Stanford University McCullough Bldg, Stanford, CA 94305-4045 USA. He is now with Silvaco International, Santa Clara, CA 95054 USA.

M. P. Anantram is with the Electrical and Computer Engineering Department, University of Waterloo, Waterloo, ON N2L 3G1, Canada.

Color versions of one or more of the figures in this paper are available online at http://ieeexplore.ieee.org.

Digital Object Identifier 10.1109/TNANO.2007.899638

1536-125X/$25.00 © 2007 IEEE

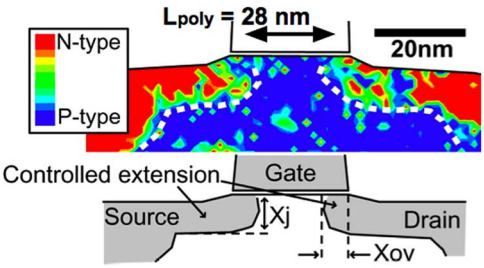


Fig. 1. Experimental carrier profile around S/D extension region in a n-MOSFET with gate length of 28 nm. The STM image was taken at negative gate bias voltage and under measuring conditions sensitive to n-type region. Overlap of S/D extension region (Xov) is about 6 nm. From [19, Fig. 9,] by permission.

most studies of doping atomicity on MOSFET performance have entailed classical simulations: the first 3-D (classical) study was made by Wong and Taur [10]; the first convincing experimental study was reported by Mizuno *et al.* [11]; and we note that one of the most cited early studies [12] utilizes 2-D MINIMOS simulations; application to deep submicrometer MOSFETs was first reported by a number of authors in the late nineties [13]–[15], again using classical methodology ranging from drift-diffusion models to Monte Carlo simulation; extensive systematic classical statistical studies of deep-submicrometer to decanano MOSFET device variability were subsequently reported in [16] and [17] and reviewed in [18]. In the present paper, for the first time, we use full quantum simulation tools to examine the importance of these fluctuations (modeled by clustering) in the doping profiles in source and drain regions that may be treated as essentially continuous but which are inhomogeneous in space.

On small enough scales the microscopic distributions are non-self-averaging; this leads to strong discrete deviations from the continuous macro-distribution. Indeed, for devices under 30 nm channel length, and even for high doping levels, it is difficult to obtain a macroscopically homogeneous distribution of dopants at the interface between the channel and source/drain regions. This is illustrated dramatically by recent scanning tunneling microscope (STM) measurements that have determined the carrier profile around the source/drain extension region of n- and p-MOSFETs with 28 nm gate length [19] as shown in Fig. 1. Although the DG-MOSFETs may be designed advantageously with nominally undoped channels, the inhomogeneity of source/drain doping is anticipated to produce discrete aggregation effects: clustering; fluctuations in the number of clusters; and fluctuations in the relative position between the clusters. Here, we are concerned with spatial fluctuations of the intended high continuous doping in source and drain and not with the resolution into individual dopants that is more typical of channel doping as described previously [6]–[18]. Previous classical studies, based on drift-diffusion modeling [20], have predicted no more than 5% variations in the on-current due to cluster number and cluster fluctuations in the source and drain of a sub-10 nm DG-MOSFETs. In this paper we show this conclusion is over-optimistic when clustering and full self-consistent quantum transport is used to model DG devices using the nonequilibrium Green function (NEGF) method [2], [21], [22].

II. The NEGF Approach Model and Computational Algorithm

The NEGF approach to carrier transport in mesoscopic systems, comes from the marriage of two old ideas due to Schwinger–Keldysh (SK) and Landauer–Buttiker (LB) [23]–[26]. The first idea, SK, was the use of propagators and correlation functions (Green's functions) to describe the motion of electrons in nonequilibrium quantum statistical systems or systems coupled to noncoherent systems such as random oscillators or reservoirs. The second idea, LB, is based on the observation that when a difference in potential is applied to a mesoscopic system, which essentially consists of two or more reservoirs connected by (short channel length and cross section) quantum channels, the same difference in the chemical potentials between the respective reservoirs is induced and this determines the current, while the electrostatic potential is allowed to float (Neumann boundary conditions) in order to fulfil charge neutrality. The current flowing between two reservoirs is controlled by (quantum) transmission in the channel connecting the reservoirs, so implicitly the reservoirs are kept with a fixed difference in chemical potential between them. Under certain simplifying assumptions [27] the current flow between two reservoirs is proportional to the transmission function and the difference of chemical potentials between the reservoirs [25], [27]. Essentially, in this approach resistance is represented by transmission [28].

In the modern NEGF formalism [21] the current and electron density in a mesoscopic system, when a difference in potential is applied, is computed by the help of the electron propagator G^R and correlation function $G^<$. The boundary conditions are included in the self-energy Σ^R (dynamic boundary condition) and statistical self-energy matrix $\Sigma^<$ (statistical boundary condition). The matrix equations (the Green functions are matrices in the coordinate representation) for the electron propagator and the correlation function may be written as [21], [29]

$$\left[G_0^{-1}-\Sigma^R\right]G^R = I \tag{1}$$

$$G^< = G^R\Sigma^< G^A \tag{2}$$

$$n(E;\mathbf{r}) = -2iG^<(E;\mathbf{r},\mathbf{r})/\pi \tag{3}$$

$$\mathbf{J}(E;\mathbf{r}) = -\frac{e\hbar}{4\pi}\mathbf{m}^{*-1}.(\nabla-\nabla')G^<(E;\mathbf{r},\mathbf{r}')|_{\mathbf{r}=\mathbf{r}'} \tag{4}$$

where $G_0^{-1} = H - i\eta$ and H is the Hamiltonian of the finite device; Σ^R contains the effect of the injecting and absorbing (IA) boundaries on the open system. The statistical self-energy matrix $\Sigma^<$ is given by the imaginary part of the self-energy for each IA boundary multiplied by the distribution function at the boundary value of the chemical potential (including the external potential). Scattering is not considered. $iG^<(E;r,r)$ or $n(E;r)$ are the density of electrons at the position r with energy E; $\boldsymbol{J}$ is the energy-resolved current density associated with electrons of energy E. The total electron density is obtained by integrating (3) over all energies. Expression (4) also should be integrated for all energies to give the total current density. The electron density must satisfy Poisson's equation; therefore, a self-consistent iterative cycle is set up to compute the electron density and potential throughout the device.

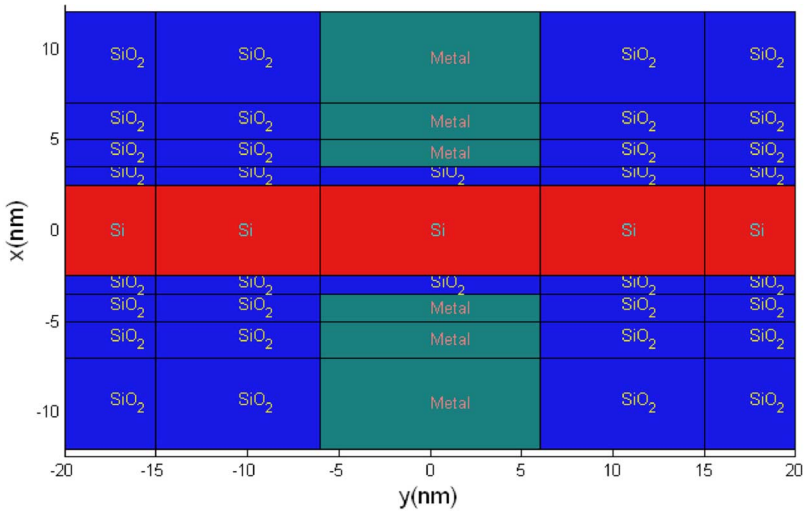


Fig. 2. Double-gate MOSFET structure (DG-MOSFET).

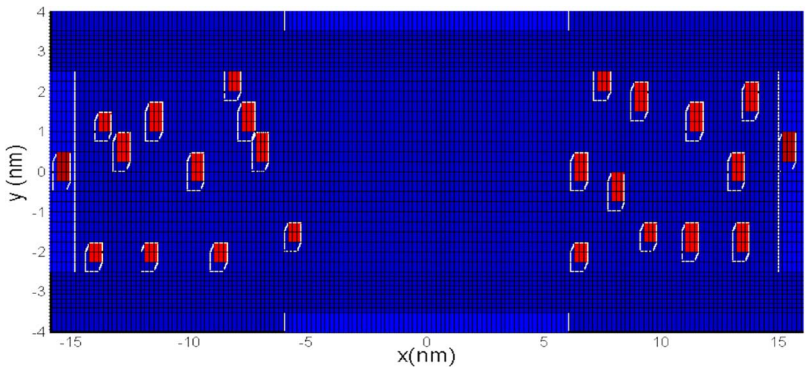


Fig. 3. Simulation domain, showing nonuniform spatial grid and high doping emplacements.

As can be seen from (3) and (4), we only need to calculate the diagonal and off-diagonal elements of the $G^<$ function in order to compute the current and electron density. For this purpose we deploy a recursive algorithm technique based on the symmetry of the Dyson equation, which allows us to compute the diagonal, and off-diagonal blocks of $G^<$ without the need to invert the Hamiltonian matrix of the whole device. A very detailed description of the recursive algorithm used in this work may be found in [22].

III. Device Geometry and Dopant Model

Fig. 2 shows the structure of the simulated silicon DG-MOSFET with a channel length of 12 nm and a channel thickness of 5 nm. The oxide thickness is 2 nm. The average n-type doping concentration in the source/drain is $\langle n_{3D} \rangle = 10^{20}$ cm^{-3}; the channel is undoped. The dopant model adopted here utilizes a Poissonian clustering scheme confined to a region of 9 nm before and after the channel, outside which the doping is considered to be uniform since sufficient numbers of dopants exist for self-averaging (consistent with findings reported in [19]). The average continuum doping is fixed at 10^{20} cm^{-3}. Fig. 3 illustrates the simulation domain showing the nonuniform spatial mesh, undoped channel, discrete source and drain regions, and the surrounding continuum model regime.

The clusters of dopants are modeled by small randomly located regions of very high continuous doping concentration normalized to fit the average density in the clustered source/drain region to the uniform source and drain doping. The doping fluctuations represented by the clustering are of the order of 10% of the average doping level consistent with experimental data [19]. It is important to stress that the individual impurities are not spatially resolved in the model. Indeed, the full self-consistent potential landscape smoothes out considerably around the cluster positions (see Figs. 4 and 5). The device is assumed to be very wide so that it may be modeled in two dimensions following [22]. The clusters of high doping regions have a 2-D character in the sense that we are assuming that in the direction perpendicular to the device plane the doping inhomogeneities became less severe and therefore restore the lateral symmetry of our problem. Hence, we assume, as a first approximation, that the fluctuation are more severe in the device plane and therefore we neglect on average the fluctuations in the perpendicular direction. The intended doping in a smooth device goes from 1×10^{20} cm^{-3} to zero in a few nanometers in the transport direction but in the off-plane direction the doping remains constant. Therefore, it is natural to expect more fluctuations in the plane of the device. With the present state of the art in Green function algorithms a 3-D analysis of this clustering by a full 3-D NEGF simulator is virtually impossible in a DG-MOSFET context because of the required high spatial complexity. Even

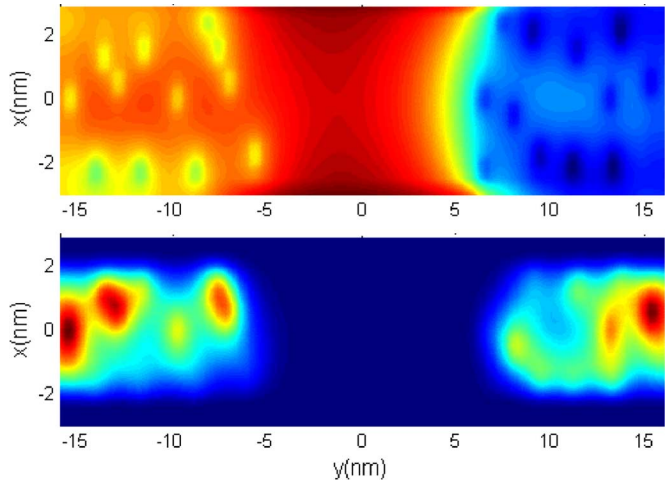


Fig. 4. Spatial profile of potential (upper panel) and electron concentration (lower panel) in the source, channel and drain regions of a 12 nm channel length DG-MOSFET for the dopant aggregation configuration shown in Fig. 6 (upper panel). Average doping concentration in $S/D = 10^{20}$ cm^{-3}, number of high doping clusters $\langle N \rangle = 10$; actual number of high doping clusters $N = 12$.

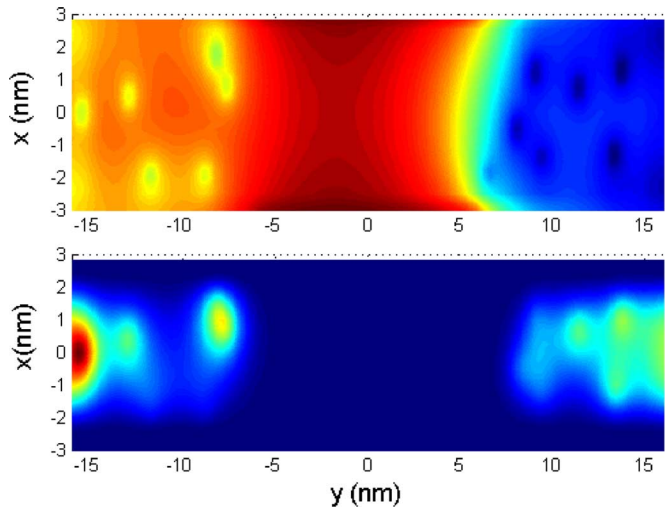


Fig. 5. Spatial profile of potential (upper panel) and electron concentration (lower panel) in the source, channel and drain regions of a 12 nm channel length DG-MOSFET for the dopant aggregation configuration shown in Fig. 6 (lower panel). Average doping concentration in $S/D = 10^{20}$ cm^{-3}, number of high doping clusters $\langle N \rangle = 10$; actual number of high doping clusters $N = 6$.

if this could be done, and certainly if mode space reduction schemes can be validated the work reported here will be relevant as a comparison, because the 2-D simulation is much less computationally expensive. The doping inhomogeneities are schematized in Fig. 3 by the box representation. From a 2-D viewpoint the 2-D clusters have an average concentration $\langle n_{2D} \rangle = \langle n_{3D} \rangle^{2/3} \approx 2.5 \times 10^{13}$ cm^{-2}. It follows that there are approximately $N \approx 10$ clusters in each of the source and drain discrete doping regions.

We have simulated several devices that differ in the cluster spatial configurations for the case $\Delta N = 0$, and for the case $\Delta N \neq 0$ that describes fluctuations in total cluster number. The ensemble of devices with fluctuating numbers of clusters was constructed from a Gaussian distribution centred on the mean dopant number derived from the average doping concentration in source/drain respectively.

The transport is treated as ballistic because of the relatively short channel length. Here, we use the term ballistic to indicate in particular that dissipative (energy-relaxing) processes are neglected. We also neglect the contributions to the self-energy in the source and drain regions due to scattering on individual dopants which are not spatially resolved in our model. This latter ballistic approximation for source and drain has been utilized elsewhere in quantum transport calculations for nanowires and MOSFETs [22], [30]–[32]. The treatment of carrier interaction with the essentially classical clusters in the continuous doping profile and with the boundaries is treated nonperturbatively by folding the total self-consistent electrostatic potential landscape into the device Hamiltonian. In the absence of clustering the model reduces to the commonly accepted homogeneous doping model [22], [30]–[32] for DG and nanowire devices that are nominally undoped in the channel. When doping fluctuations in source and drain generate clustering effects, as reported experimentally [19], the principal effects are in the charge injection and extraction. Our model specifically excludes scattering on individual atomistic dopants. Tunneling processes are automatically included nonperturbatively. Self-consistency is achieved by coupling the transport to the total electrostatic potential via the electron density and Poisson's equation.

We observe that if a microscopic model of discrete dopants were to be deployed then for a uniformily doped high density region self-averaging will occur, leading to the validation of the Kohn–Luttinger *ansatz* for the existence of a self-energy for impurity scattering to which we have already alluded. However, the strong, countable nonuniformities in doping discussed here will give rise to additional but weaker scattering processes but these will not be describable by a self-energy since the Kohn–Luttinger *ansatz* fails [2], [4], [5] for small finite numbers of scattering centers: the self-energy is real and the scattering processes are nondissipative in the sense of being time-reversible. *A fortiori*, this is the case for small numbers of individual dopants such as the unintentional atomistic doping in the channel and it also applies to the source/drain extension inhomogeneities. Rather, these weak additional interactions will appear as time-reversible processes which are fully described within the ballistic Green function model.

IV. Simulation Results

To set the background for the device characteristics we first present the potential distribution of one of the devices with a random distribution of clusters (upper panel of Fig. 4). The corresponding electron distribution in the channel and the discrete dopant aggregation regime (clustering) of source and drain is shown in the lower panel of Fig. 4. Similar data is shown in Fig. 5 but for fewer clusters (i.e., an effective lower average doping). The corresponding configurations of the clusters are presented in Fig. 6 (the upper panel corresponds to Fig. 4; the lower panel corresponds to Fig. 5).

Fig. 7 shows the $I_D - V_G$ characteristics for five devices that differ only in the arrangement of clusters $(\Delta N = 0)$. Data for the case of uniform continuum doping (smooth doping distribution) is included for comparison. Fig. 8 shows two cluster configurations with the same number of dopants corresponding to Fig. 7.

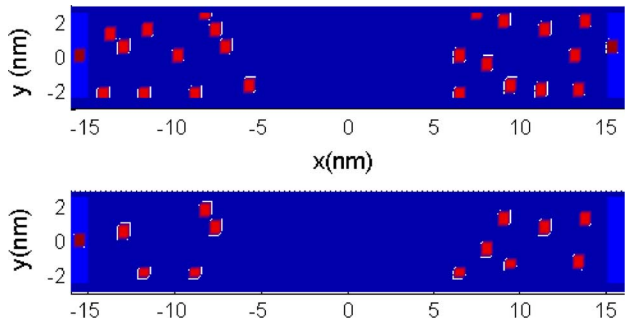


Fig. 6. Doping cluster aggregation map for DG-MOSFET source and drain regions. Upper panel: the high doping configuration corresponding to Fig. 4. Lower panel: high doping configuration corresponding to Fig. 5.

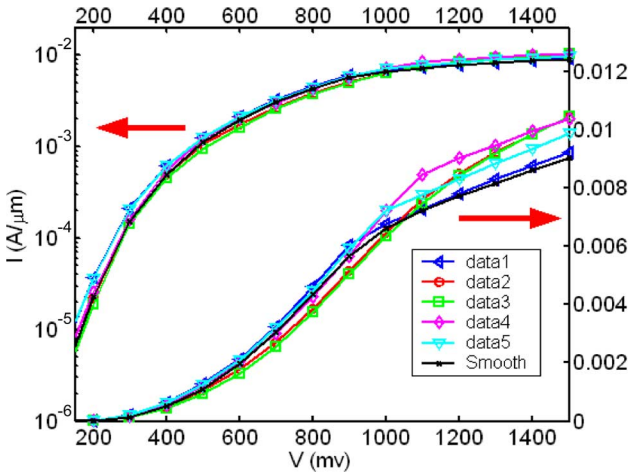


Fig. 7. Computed I_D–V_G characteristics of devices that differ only in the arrangement of high doping clusters $(\Delta N = 0)$.

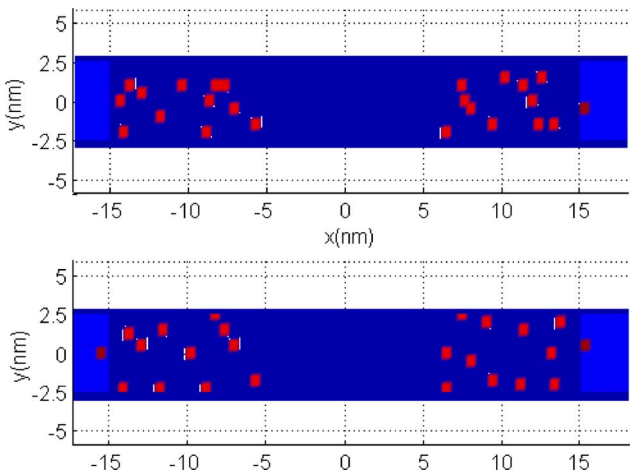


Fig. 8. Two high doping configurations with the same number of clusters corresponding to Fig. 6.

Fig. 9 shows the $I_D - V_G$ characteristics for a different number of total clusters $(\Delta N \neq 0)$ ranging from 13 to 35 discrete cluster locations. Again, data for the case of continuum doping (smooth doping distribution) is included for comparison.

In Fig. 10 we exhibit the current density J_x (lower panel) through the self-consistent potential landscape (upper panel) corresponding to the device with the doping configuration shown in the lower panel of Fig. 7.

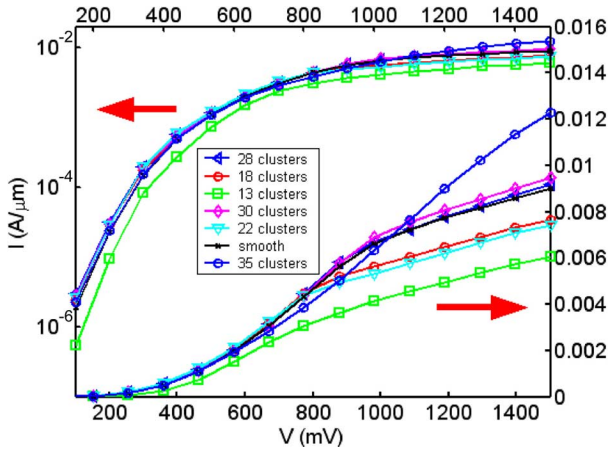


Fig. 9. Computed I_D–V_G characteristics of devices that differ in the arrangement of high doping clusters and in fluctuations of doping cluster number $(\Delta N \neq 0)$.

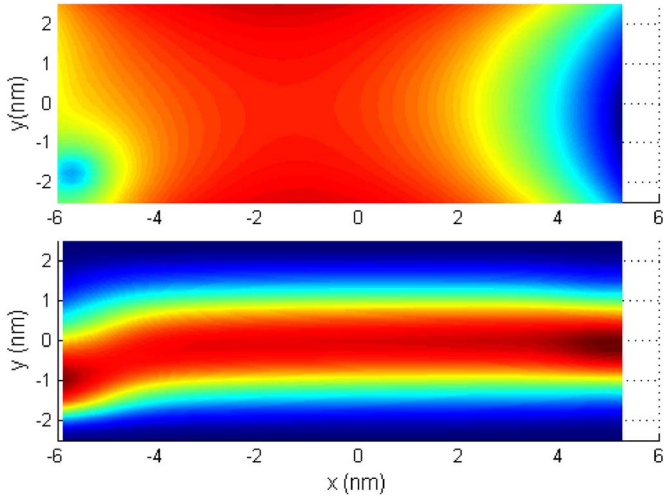


Fig. 10. Potential and current density landscapes corresponding to the device with the high doping configuration of the lower panel in Fig. 7. Upper panel: potential landscape. Lower panel: current density long the channel.

V. Discussion and Conclusion

From Figs. 4, 5, and 7 it may be seen as anticipated that the self-consistent potential landscape effectively obscures the bare cluster potentials. It should be stressed that this result is a consequence of the thermal averaging (at 300 K) over the quasi-continuum of energy states inherent in the Green function simulation. Sharper features are found in the spectrally resolved Green functions which lead to complex features in the energy-resolved electron concentration. The total electron concentration and hence the total self-consistent potential distribution results from the thermal average of which obscures many of the obvious quantum effects in. However, full self-averaging does not take place and the source and drain regions, for example, exhibit inhomogeneous potential distributions and carrier distributions. The granularity of the carrier distribution has a strong resemblance to the experimental data of Fig. 1, albeit for a much shorter device channel.

Fig. 10 shows the typical result that, despite the uniform undoped channel, the current meanders through the channel; the flow is nonuniform. This is a direct result of the inhomogeneous injection through the random potential landscape of the

source; it is characteristic of spatially inhomogeneous doping resolved structures similar to atomistically resolved structures [2]–[5]. The resulting injected current flow is reflected from the walls of the channel. The spatial characteristics of the flow are different from classical modeling: the transport is thermodynamic quantum transport. The spectrally resolved current density along the channel shows more complex behavior, consistent with channel quantization, but the total current density is smoothed by the thermal average over the energy states E. No trace of the characteristic quantized current response found at low temperatures is found at electron temperatures Te $\geq$ 300 K. However, the monotonic current–voltage characteristics display quite different values for threshold voltage, subthreshold response and on-current response from the classical results [20].

Comparing Figs. 5 and 6 we find that the fluctuation in total number of dopants has a stronger effect (50% fluctuation in on-current) than purely positional fluctuations of the clusters (10%). In both cases the impact on the on-current is stronger than the effect on the subthreshold response. The computed on-current fluctuations are significantly larger than the classical predictions [20]. We conclude that for practical device design it is crucial to control precisely the total number of dopants $(\Delta N \rightarrow 0)$ in the source and drain to avoid large performance fluctuations.

For the first time this work has explored the effects of the doping inhomogeneity in the source/drain regions revealed recently in experiments [19] using a 2-D NEGF formalism in a DG-MOSFET. As the STM experiments show [19], the existence of clustering and aggregation are likely to appear around the end terminations. This clearly affects the injection of carriers in the channel of the device, and creates fluctuations from device to device as has been show in our calculations. In this study we have not included the effects of unintended atomistic dopants in the channel or atomically resolved dopants close to the source/drain interfaces with the channel. As discussed in previous studies [2]–[5] atomistically resolved dopants generally require 3-D modeling.

In this work, symmetry in the perpendicular direction is assumed and all the physical magnitudes have lateral symmetry reflected in the 2-D electrostatics as a logarithmic dependence of the potential as a function of coordinates. This is the case in every 2-D simulation. An analysis in three dimensions of 3-D doping inhomogeneities is beyond the scope of this work. Even so, a 3-D analysis could be more relevant for bulk MOSFETs (three spatial dimensions of the device in the same order of magnitude) with intrinsically 3-D character. This type of analysis for DG-MOSFET will require a very large 3-D model in order to avoid the effect of the lateral boundaries and to be able to restore the global lateral symmetry. A 3-D NEGF description of this device is computationally complex and will be addressed it in a future work.

Finally, we note that one of the motivations for utilizing the Green function formalism rather than a self-consistent Schrödinger wave equation solver is that the NEGF formalism provides a firm basis for the future inclusion of energy relaxation, hot electron and many-body effects such as dynamic screening and the interacting carrier assembly.

But perhaps the most practical feature of the Green function approach is the use of simple contact self-energies that permit modeling of open systems by finite boundary methodology. The Green function approach may be regarded as having the same role as ensemble Monte Carlo has in the classical modeling of devices. That is, it provides a secure underpinning for the validation of more efficient, but approximate modeling schemes. These aspects will be addressed in future work.

ACKNOWLEDGMENT

The authors would like to thank A. Brown for his enlightening discussions and technical support in the preparation of this work.

REFERENCES

[1] International Technology Road Map for Semiconductors [Online]. Available: http://www.public.itrs.net/

[2] J. R. Barker, A. Martinez, A. Svizhenko, A. Anantram, and A. Asenov, "Green function study of quantum transport in ultra-small devices with embedded atomistic cluster," *J. Phys., Conf. Ser.*, vol. 35, pp. 233–246, 2006.

[3] A. Martinez, A. Svizhenko, M. P. Anatram, J. R. Barker, and A. Asenov, "A study of the effect of interface roughness on a DG-MOSFET using full 2D NEGF technique," in *IEDM Tech. Dig.*, 2005, pp. 627–630.

[4] J. R. Barker, "A theoretical study of atomistic effects on the quantum hydrodynamics of carriers in decanano semiconductor devices using non-self-averaged Green functions," *Physica*, vol. E19, pp. 62–70, 2003.

[5] J. R. Barker, "Non-equilibrium quantum transport in finite device structures in the presence of non-self-averaged atomistic impurity scattering," *Semicond. Sci. Technol.*, vol. 19S, pp. 56–59, 2004.

[6] R. W. Keyes, "Effect of randomness in the distribution of impurity ions on FET thresholds in integrated electronics," *IEEE J. Solid-State Circuits*, pp. 245–247, 1975.

[7] J. A. Nixon, J. H. Davies, and J. R. Barker, "Fluctuations in sub-micron semiconducting devices caused by the random position of dopants," in *Physics and Fabrication of Nanostructures*, M. Read and W. P. Kirk, Eds. New York: Academic, 1989, pp. 123–127.

[8] J. A. Nixon and J. H. Davies, "Potential fluctuations in heterostructure devices," *Phys. Rev. B*, vol. 41, pp. 7929–7932, 1990.

[9] M. J. Laughton, J. R. Barker, J. A. Nixon, and J. H. Davies, "Modal analysis of transport through quantum point contacts using realistic potentials," *Phys. Rev. B*, vol. 44, pp. 1150–1153, 1991.

[10] H. S. Wong and Y. Taur, "Three-dimensional 'atomistic' simulation of discrete random dopant distribution effects in sub-0.1 μm MOSFET's," in *IEDM Dig. Tech. Papers*, 1993, pp. 705–708.

[11] T. Mizuno, J. Okamura, and A. Toriumi, "Experimental study of threshold voltage fluctuation due to statistical variation of channel dopant number in MOSFET's," *IEEE Trans. Electron Devices*, vol. 41, no. 11, pp. 2216–2221, Nov. 1994.

[12] P. A. Stolk and D. B. M. Klaasen, "The effect of statistical dopant fluctuations on MOS device performance," in *IEDM Dig. Tech. Papers*, 1996, pp. 627–630.

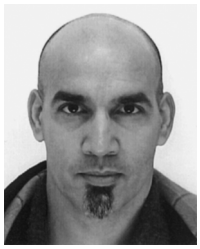
[13] H.-S. P. Wong, Y. Taur, and D. J. Frank, "Discrete random dopant distribution effects in nanometer-scale MOSFETs," *Microelectron. Reliabil.*, vol. 38, pp. 1447–1456, 1998.

[14] A. Asenov, "Random dopant induced threshold voltage lowering and fluctuations in sub-0.1 μm MOSFET's; A 3-D 'atomistic' simulation study," *IEEE Trans. Electron Devices*, vol. 45, no. 12, pp. 2505–2513, Dec. 1998.

[15] D. Vasileska, W. J. Gross, and D. K. Ferry, "Modeling of deep-submicrometer MOSFETs: random impurity effects, threshold voltage shifts and gate capacitance attenuation," in *Extended Abstracts 1998 6th Int. Workshop Computational Electronics (IWCE-6)*, pp. 259–262.

[16] A. Asenov and S. Saini, "Polysilicon gate enhancement of the random dopant induced threshold voltage fluctuations in sub-100nm MOSFET's with ultrathin gate oxide," *IEEE Trans. Electron Devices*, vol. 47, no. 4, pp. 805–812, Apr. 2001.

[17] A. Asenov, G. Slavcheva, A. R. Brown, J. H. Davies, and S. Saini, "Increase in the random dopant induced threshold fluctuations and lowering in sub-100 nm MOSFETs due to quantum effects: A 3-D density-gradient simulation study," *IEEE Trans. Electron Devices*, vol. 48, no. 4, pp. 722–729, Apr. 2001.
[18] A. Asenov, A. R. Brown, J. H. Davies, S. Kaya, and G. Slavcheva, "Simulation of intrinsic parameter fluctuations in decananometer and nanometer-scale MOSFETs," *IEEE Trans. Electron Devices*, vol. 50, no. 9, pp. 1837–1852, Sep. 2003.
[19] H. Fukutome, Y. Momiyama, E. Yoshida, M. Okuno, T. Itakura, and T. Aoyama, "Direct measurement of carrier profiles in operating sub-30-nm N-MOSFETs," in *IEDM Tech. Dig.*, 2005, pp. 57–60.
[20] A. R. Brown, A. Asenov, and J. R. Watling, "Intrinsic fluctuations in sub 10-nm double-gate MOSFETs introduced by discreteness of charge and matter," *IEEE Trans. Nanotechnol.*, vol. 1, no. 4, pp. 195–200, Dec. 2002.
[21] R. Lake, G. Klimeck, R. C. Bowen, and D. Jovanovic, "Single and multiband modeling of quantum electron transport through layered semiconductor devices," *J. App. Phys.*, vol. 81, pp. 7845–7869, 1997.
[22] A. Svizhenko, M. P. Anatram, T. R. Govindan, B. Biegel, and R. Venugopal, "Two dimensional quantum mechanical modeling of nanotransistors," *J. App. Phys.*, vol. 91, pp. 2343–2354, 2002.
[23] J. Schwinger, "Brownian motion of a quantum oscillator," *J. Math. Phys.*, vol. 2, pp. 407–432, 1961.
[24] L. V. Keldysh, "Diagram technique for non-equilibrium processes," *Sov. Phys.-JEPT*, vol. 20, pp. 1018–1026, 1965.
[25] R. Landauer, "Electrical resistance of disordered one-dimensional lattices," *Phil. Mag.*, vol. 21, pp. 863–867, 1970.
[26] M. Buttiker, "Symmetry of electrical conduction," *IBM J. Res. Dev.*, vol. 32, pp. 317–334, 1988.
[27] H. L. Engquist and P. L. Anderson, "Definition and measurement of the electrical and thermal resistances," *Phys. Rev. B*, vol. 24, pp. 1151–1154, 1981.
[28] Y. Imry and R. Landauer, "Conductance viewed as transmission," *Rev. Mod. Phys*, vol. 71, pp. S306–S312, 1999.
[29] S. Datta, *Electronic Transport in Mesoscopic Systems*. Cambridge, U.K.: Cambridge Univ. Press, 1995.
[30] M. Bescond, J.-L. Autran, N. Cavassilas, D. Munteaunu, and M. Lannoo, "Treatment of point defects in nanowire MOSFETs using the nonequilibrium Green's function formalism," *J. Comput. Electron.*, vol. 3, pp. 393–396, 2004.
[31] M. Bescond, N. Cavassilas, K. Kalna, K. Nehari, J. L. Autran, M. Lannoo, and A. Asenov, "Simulation study of performance limits for Si, Ge, and GaAs ballistic nanowire MOSFETs," in *Proc. 2005 Silicon Nanoelectronics Workshop*, M. Tabe, Ed., pp. 8–9.
[32] M. Bescond, N. Cavassilas, K. Kalna, K. Nehari, L. Raymond, J. L. Autran, M. Lannoo, and A. Asenov, "Ballistic transport in Si, Ge, and GaAs nanowire MOSFETs," in *IEDM Tech. Dig.*, 2005, pp. 526–529.



Antonio Martinez received the M.Sc. degree in physics from the University of Havana, Cuba, in 1987, the M.Sc. degree in physics from the University of Umea, Sweden, In 1997, and the Ph.D. degree from the Royal Institute of Technology, Stockholm, Sweden, in 2003. His Ph.D. thesis deals with electron transport in anisotropic materials (SiC, GaN) at high electric field using various simulation techniques as drift-diffusion, ensemble Monte Carlo, and quantum Monte Carlo.

He is currently a member of Device Modelling Group at Department of Electronics and Electrical Engineering, University of Glasgow, Glasgow, U.K. His experience includes Monte Carlo simulation technique for electron and hole transport, and nanoscale quantum electron transport using a full 3-D nonequilibrium Green's function approach, specifically simulation of nanoscale MOSFET and nanowire transistors.



John R. Barker is a graduate of the University of Edinburgh and the University of Durham. He obtained his PhD in Theoretical Physics from the University of Warwick in 1969 where he held a Personal SRC Fellowship.

From 1970 to 1985 he was a Lecturer then Senior Lecturer in Theoretical Physics at the University of Warwick, Coventry, U.K. He has been Professor of Electronics at the University of Glasgow, Glasgow, U.K., since 1985, where he was a cofounder of the Nanoelectronics Research Centre with responsibility for theory and modeling activities. He has been a Visiting Professor at Colorado State University, North Texas State University, Visiting Scientist at the IBM T. J. Watson Laboratories, and Visiting Scientist at the Niels Bohr Institute and Paris University VII. He has over 300 publications in semiconductor physics, hot electron theory, quantum transport theory, Monte Carlo simulation, device physics and modeling, quantum theory of atomistic effects in ultra-small devices, parallel computing, olfactory sensors, and molecular electronics. He has given more than 160 invited talks at international conferences and meetings in Europe, the United States, and Japan. He has a broad range of research interests that currently include nonequilibrium Green function modeling of nano-devices, silicon-germanium hetero-MOS, interface roughness modeling, smart dust, and highly parallel computer architectures.

Prof. Barker is a Fellow of the Royal Society of Edinburgh and a Fellow of the Royal Astronomical Society. He has served on a number of EPSRC/SERC national committees including Chairman of the SERC Molecular Electronics Committee and membership of SERC/DTI National Committee on Superconductivity, SERC Electronic Devices Committee, Materials Commission, and Electronic Materials Committee. He has performed consultancy work for a large number of U.K., European, and U.S. industrial and government laboratories and acted as a consultant for the European Union DG XIII Information Technology Division. He has chaired and codirected a number of international conferences and summer schools.



Alexei Svizhenko received the B.S. and M.S. degrees from the Moscow Institute of Physics and Technology, Moscow, Russia, in 1993 and 1995, respectively, and the Ph.D. degree in electrical engineering from the University of Nebraska, Lincoln, in 1999.

In 1999–2005 he was a Staff Scientist National Aeronautics and Space Administration (NASA) Ames Center for Nanotechnology, Moffett Field, CA. In 2005–2006, he was a Research Scientist at Stanford University. In 2006, he joined Silvaco International as a Senior TCAD engineer. His research interests are in the modeling and computation of quantum transport in nanotransistors, silicon nanowires, and carbon nanotubes.

Dr. Svizhenko was the recipient of the 2000 NASA Group Achievment Award and the 2003 and 2004 Computer Sciences Corporation (CSC) Best Paper Award.



M. P. Anantram received the B.Sc. degree in applied sciences from the P.S. G. College of Technology, India, in 1986, the M.Sc. degree in physics from the University of Pune, India, in 1989, and the Ph.D. degree from Purdue University, West Lafayette, IN, in 1995.

He was a Postdoctoral Fellow working on physical models of computing at Purdue University and the University of California, Los Angeles. He has been a Scientist at the NASA Ames Research Center, Mottfet Field, CA, from 1997 to 2006, and he is currently Professor at the University of Waterloo, ON, Canada. His main research focus is modeling and theory of semiconductor and molecular nanostructures, such as nanotransistors, carbon nanotubes, and DNA.

Dr Anantram received the S. S. Joshi Award for academic exellence in 1989, the Veridian Technical Award for the best paper, in 2000 for work on the electromechanical properties of carbon nanotubes, the NASA Group Achievement Award to the Nanotechnology Team, the CSC best paper award in 2002, for work on the electromechanical properties of carbon nanotubes, and the 2003 CSC Technical Excellence Award for work on modeling and theory of nanostructure.



Asen Asenov (M'96) received the M.Sc. degree in solid-state physics from Sofia University, Bulgaria, in 1979 and the Ph.D. degree in physics from the Bulgarian Academy of Science, Sofia, in 1989.

He had ten years industrial experience as a head of the Process and Device Modelling Group at IME-Sofia, developing one of the first integrated process and device CMOS simulators IMPEDANCE. In 1989–1991 he was a visiting professor at the Physics Department of TU Munich. He joined the Department of Electronics and Electrical Engineering at the University of Glasgow in 1991 and served as a Head of Department in 1999–2003. As a Professor of Device Modelling, leader of the Glasgow Device Modelling Group, and academic director of the Glasgow Process and Device Simulation Centre, he coordinates the development of 2-D and 3-D quantum mechanical, Monte Carlo, and classical device simulators and their application in the design of advanced and novel CMOS devices. He has pioneered the simulations and the study of various sources of intrinsic parameter fluctuations in decanano and nano CMOS devices including random dopants, interface roughness, and line edge roughness.

Prof. Asenov is a Fellow of the Royal Society of Edinburgh and a member of the IEEE EDS TCAD Committee. He is currently a member of the program committees for IEDM, ESSDERC, IWCE, SNW, HCIS, and IEEE Nano Conf, and SNW2006. He has over 330 publications in semiconductor device physics on process and device modeling and simulation. He is an expert on atomistic effects in ultrasmall devices and impact of variations on circuits and systems including more than 15 papers in IEEE TRANSACTIONS ON ELECTRON DEVICES in the last five years. He has also given more than 65 invited talks at prestigious international conferences and meetings in Europe, the United States, and Japan.